

Title: Mixed-potential-driven catalysis

Authors: Mo Yan¹†, Kotaro Takeyasu^{2,3,4*}†, Nuning A. P. Namari¹, Junji Nakamura^{3,4,5}

Affiliations:

¹Graduate School of Science and Technology, University of Tsukuba; 1-1-1 Tennodai, Tsukuba, Ibaraki 305-8573, Japan.

²Department of Materials Science, Faculty of Pure and Applied Sciences, University of Tsukuba; 1-1-1 Tennodai, Tsukuba, Ibaraki 305-8573, Japan.

³Tsukuba Research Centre for Energy and Materials Science, University of Tsukuba; 1-1-1 Tennodai, Tsukuba, Ibaraki 305-8573, Japan.

⁴R&D Center for Zero CO₂ Emission with Functional Materials, University of Tsukuba; 1-1-1 Tennodai, Tsukuba, Ibaraki 305-8573, Japan.

⁵Mitsui Chemicals, Inc. - Carbon Neutral Research Center (MCI-CNRC), International Institute for Carbon-Neutral Energy Research (I2CNER), Kyushu University; 744 Motoooka, Nishi-ku, Fukuoka-shi, Fukuoka 819-0395, Japan.

*Corresponding author. Email: takeyasu.kotaro.gt@u.tsukuba.ac.jp

† These authors contributed equally to this work

Abstract:

Mixed-potential-driven catalysis is expected to be a new heterogeneous catalytic mechanism that produces products different from those produced by thermal catalytic reactions without the application of external energy. Electrochemically, the mechanism is similar to that of corrosion. However, a theory that incorporates catalytic activity as a parameter has not been established. Herein, we report the theoretical framework of mixed-potential-driven catalysis, including exchange currents, as a parameter of catalytic activity. The mixed potential and partitioning of the overpotential were determined from the exchange current by applying the Butler–Volmer equation at a steady state far from equilibrium. Mixed-potential-driven catalysis is expected to open new areas not only in the concept of catalyst development but also in the field of energetics of biological enzyme reactions.

One-Sentence Summary:

Theoretical framework of mixed-potential-driven reactions in heterogeneous catalysis

Main Text:

Heterogeneous catalysis is crucial for solving various problems related to environment, energy, biology, and materials (1–4). Generally, heterogeneous catalysis occurs both thermally and electrochemically (5–7). Recently, it has been suggested that thermal heterogeneous catalysis indeed includes electrochemical processes, leading to markedly different selectivity compared to thermal catalysis (8–10). In particular, electrode reactions that form mixed potentials typified by corrosion phenomena have attracted attention. Alternatively, the anodic and cathodic half-reactions occur in pairs on a single catalyst surface, where a mixed potential is expected to form if the catalyst is electrically conductive and a suitable electrolyte is present near the active sites, as shown in **Fig. 1A**. Intriguingly, it has been reported that some heterogeneous catalytic reactions of gas molecules involve mixed-potential-driven catalysis, showing a different selectivity from normal thermal catalysis such as H₂O₂ production (9), the oxidation of formic acid (10) and hydroquinone (11), the oxidation of alcohols (hydroxymethylfurfural) (12–14), CO₂ hydrogenation (15), and 4-nitrophenol hydrogenation (16). These findings indicate that mixed-potential-driven catalysis represents a new category of heterogeneous catalysis. Because the mixed-potential-driven catalysis fundamentally changes the activity and selectivity of catalysts, it is expected to be applied to industrial catalysts in the future. However, the determining principle behind both the activity and selectivity, specifically the partitioning of the driving force for each half-reaction, has not been considered.

Mixed-potential-driven reactions have been mainly discussed in the field of electrochemistry, but not in heterogeneous catalysis. The mixed potential theory was first introduced by Wagner and Traud in 1938 in corrosion science (17). As shown in **Fig. 1B**, the basic principle can be understood in terms of the polarization curves of two electrochemical reactions described by the Butler–Volmer equation, where i_1 , i_2 and ϕ_1^{ocp} , ϕ_2^{ocp} represent the current and open circuit potential of two redox reactions $R_1 \rightleftharpoons O_1 + e^-$ and $O_2 + e^- \rightleftharpoons R_2$, with $\phi_2^{\text{ocp}} > \phi_1^{\text{ocp}}$. When the two reactions proceed concurrently, $i_1 + i_2 = 0$ is satisfied owing to the conservation of electric charge forming a mixed potential ϕ^{mix} . Here, $\phi^{\text{mix}} - \phi_1^{\text{ocp}}$ and $\phi^{\text{mix}} - \phi_2^{\text{ocp}}$ act as the overpotentials η_1 and η_2 in the two reactions (18). In the literature (19–33), mixed potentials and reaction currents have been formulated for simple pair and parallel reactions with the effects of mass diffusion. Notably, an overpotential accelerated the electrochemical reactions (33, 34). Therefore, the partitioning of the overpotential is essential because some kinetically unfavorable half-reactions can be accelerated with a high overpotential by coupling a kinetically favorable half-reaction. It is argued that to achieve the same rate, a larger overpotential is required to conduct the electrode reaction with a higher activation barrier (9). In other words, the energies of the band-electron intermediates coupling the two half-reactions are affected by changes in the electrochemical potential of the catalyst, which sets the relative driving force of each half-reaction (11). Despite advances in the understanding of the mixed-potential-driven catalysis, determining the overpotential as the driving force based on the catalytic activity has not been elucidated so far.

Mixed-potential-driven catalysis is classified as a non-equilibrium thermodynamic phenomenon. The chemical potential drop between the reactants and products becomes the driving force for the reaction, overcoming the activation energy and converting it into energy to increase the reaction rate (35). When the equilibrium state is achieved, the driving force becomes zero, which is converted to the heat of reaction (36). Prigogine constructed a theoretical framework based on entropy change to conserve the energy (37, 38). However, it has not been explicitly stated that $d_i S$

(entropy production) corresponds to the overpotentials that promote the reaction in the case of mixed-potential-driven catalysis. Discussion of the entropy change with this overpotential is essential for discussing the reaction rate. In this paper, we extend Prigogine's theory to the mixed-potential-driven catalysis and present the kinetic equations. Enzymatic reaction systems in living organisms, such as glucose oxidase and lactate oxidase, may also proceed via a mixed-potential-driven reaction, in which the anodic and cathodic reactions are paired (39–43). Thus, the framework of mixed-potential-driven catalysis is fundamental for considering the energy pathways of how entropy is generated in the body, which is used to drive metabolic reactions, maintain body temperature as heat, and dissipated outside. The non-equilibrium theory of mixed-potential-driven reactions is expected to improve our understanding of the energetics of biological systems.

In this study, we present a new equation for the conversion of the Gibbs free energy drop between the cathodic and anodic reactions into overpotentials by the formation of a mixed potential. In particular, the equation explains how the catalytic activity plays a pivotal role in determining the mixed potential, overpotentials, reaction current, and selection of the cathodic and anodic reactions. This is the equation for the new concept of mixed-potential-driven catalysis. This concept is important in the development of kinetically difficult catalytic reactions, understanding the energy transfer of enzymatic reactions in living organisms, and in the non-equilibrium theory of chemical reactions.

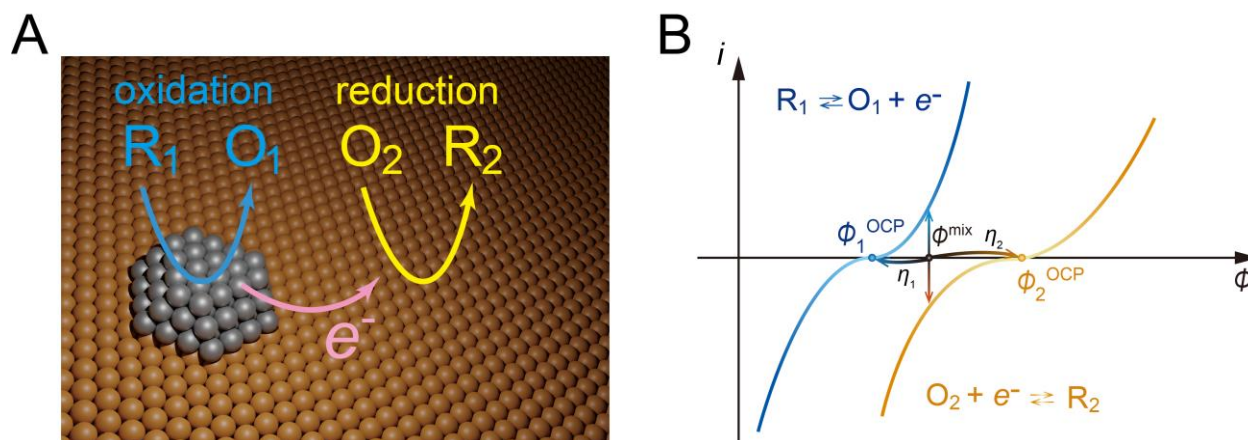


Fig. 1. A typical mixed-potential-driven reaction. (A) Electrons released in the oxidation reaction from reductant R_1 to oxidant O_1 are used in the reduction reaction from oxidant O_2 to reductant R_2 . (B) Illustrative polarization curves for the cathodic and anodic half-reactions. The mixed potential is the point at which the net of the cathodic and anodic currents is zero.

Driving force of mixed-potential-driven catalysis

First, we show how the total driving force of the entire mixed-potential-driven catalytic reaction system is distributed to the overpotentials for accelerating the anodic and cathodic half-reactions, depending on the catalytic activity of the catalysts. For simplicity, we consider a mixed potential system, as shown in Fig. 2A, where anodic reaction 1 and cathodic reaction 2 can occur in both components I and II of the catalyst, so that four types of electron transfer are possible.

Reaction 1: $R_1 \rightleftharpoons O_1 + e^-$	(1)
Reaction 2: $O_2 + e^- \rightleftharpoons R_2$	(2)

The net reaction is expressed by the following equation.



Electrochemically, microelectrodes I and II can be regarded as short-circuited, with both electrodes exposed to identical gas or liquid conditions, regardless of whether they are spatially separated. Unlike ordinary electrochemical cells, the distinction between the anode and cathode is not fixed before starting the reaction. Consequently, the reaction 1 and 2 can take place on each of catalyst components I and II, where one assumes that open circuit potential of reaction 1 (ϕ_1^{ocp}) is lower than that of reaction 2 (ϕ_2^{ocp}). The potential difference of $\phi_2^{\text{ocp}} - \phi_1^{\text{ocp}}$ corresponds to the total driving force of the net reaction Equation 3.

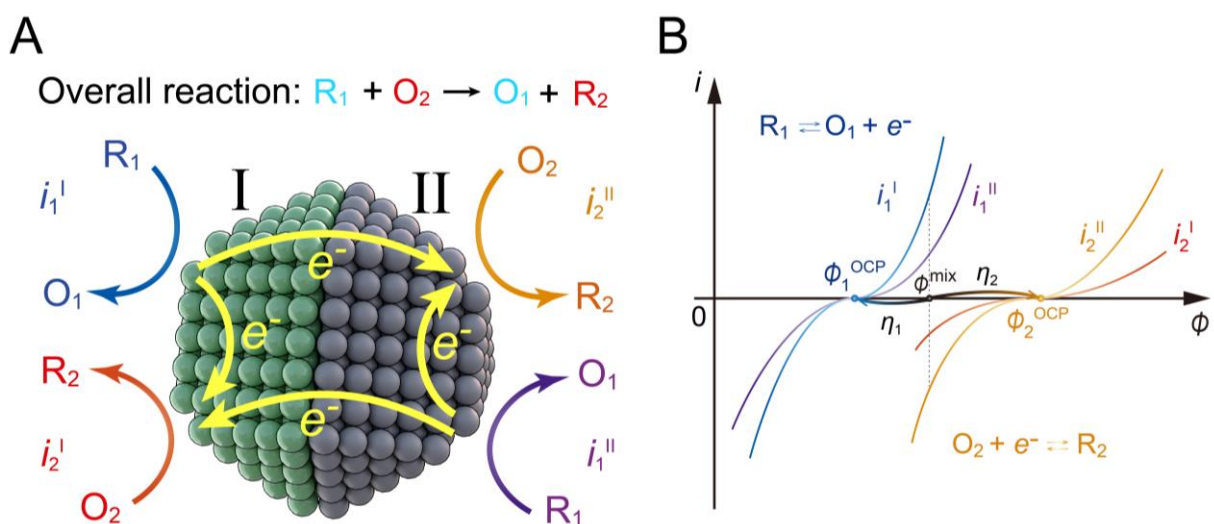


Fig. 2. Proposed mixed-potential-driven catalysis model. (A) Schematic of a mixed-potential-driven catalytic reaction occurring on the catalyst composed of component I and II. Cathodic and anodic half-reactions can occur in each of the component I and II. Electrons are transferred within and between the component I and II. (B) Illustration of the four polarization curves for the cathodic and anodic half-reactions on catalyst component I and II. The mixed potential is the point at which the sum of the four currents is zero.

To estimate the mixed potential and current at the mixed potential, it is necessary to analyze the polarization curve, which depends on the catalytic activity and is expressed by the Butler–Volmer equation. The currents of the electrochemical half-reactions (1) and (2) on component I are given by the Butler–Volmer equation with no mass-transfer effect:

$$i_1^I = i_1^{I0} \left(e^{(1-\alpha_1)f(\phi^{\text{mix}} - \phi_1^{\text{ocp}})} - e^{-\alpha_1 f(\phi^{\text{mix}} - \phi_1^{\text{ocp}})} \right) \quad (4)$$

$$i_2^I = i_2^{I0} \left(e^{(1-\alpha_2)f(\phi^{\text{mix}} - \phi_2^{\text{ocp}})} - e^{-\alpha_2 f(\phi^{\text{mix}} - \phi_2^{\text{ocp}})} \right) \quad (5)$$

where $f = F/RT$ and F , R , and T are the Faraday constant, gas constant, and temperature, respectively. α_1 and α_2 are the transfer coefficients for reaction 1 and reaction 2, respectively. i_1^{I0} and i_2^{I0} are the exchange currents for reactions 1 and 2 in component I, respectively. The exchange current i^0 corresponds to the catalytic activity and determines the shape of the polarization curve

(44). For Butler–Volmer equations on component II, "I" in Equations (4) and (5) shall be replaced by "II." As shown in **Fig. 2B**, once a mixed potential is formed, the net current is zero according to the definition of the mixed potential (17).

$$i_1^I + i_1^{II} + i_2^I + i_2^{II} = 0 \quad (6)$$

Substituting the equations of currents on component I and II into Equation (6) and assuming $\alpha_1 = \alpha_2 = \alpha$, we can obtain a mixed potential of ϕ^{mix} at the steady-state of reaction as follows:

$$\phi^{\text{mix}} = \frac{1}{f} \ln \frac{(i_1^{I0} + i_1^{II0}) e^{\alpha f \phi_1^{\text{ocp}}} + (i_2^{I0} + i_2^{II0}) e^{\alpha f \phi_2^{\text{ocp}}}}{(i_1^{I0} + i_1^{II0}) e^{-(1-\alpha)f \phi_1^{\text{ocp}}} + (i_2^{I0} + i_2^{II0}) e^{-(1-\alpha)f \phi_2^{\text{ocp}}}} \quad (7)$$

The absolute value of the anodic and cathodic currents must be the same, which is the current at the mixed potential (i^{mix}) for the net reaction.

$$i^{\text{mix}} = |i_1^I + i_1^{II}| = |i_2^I + i_2^{II}| \quad (8)$$

Substituting Equation (7) into Equations (4), (5), and (8) gives i^{mix} .

$$\begin{aligned} i^{\text{mix}} &= (i_1^{I0} + i_1^{II0}) \left(e^{(1-\alpha)f(\phi^{\text{mix}} - \phi_1^{\text{ocp}})} - e^{-\alpha f(\phi^{\text{mix}} - \phi_1^{\text{ocp}})} \right) \\ &= (i_1^{I0} + i_1^{II0}) \left[\left(\frac{(i_1^{I0} + i_1^{II0}) + (i_2^{I0} + i_2^{II0}) e^{\alpha f(\phi_2^{\text{ocp}} - \phi_1^{\text{ocp}})}}{(i_1^{I0} + i_1^{II0}) + (i_2^{I0} + i_2^{II0}) e^{-(1-\alpha)f(\phi_2^{\text{ocp}} - \phi_1^{\text{ocp}})}} \right)^{1-\alpha} \right. \\ &\quad \left. - \left(\frac{(i_1^{I0} + i_1^{II0}) + (i_2^{I0} + i_2^{II0}) e^{\alpha f(\phi_2^{\text{ocp}} - \phi_1^{\text{ocp}})}}{(i_1^{I0} + i_1^{II0}) + (i_2^{I0} + i_2^{II0}) e^{-(1-\alpha)f(\phi_2^{\text{ocp}} - \phi_1^{\text{ocp}})}} \right)^{-\alpha} \right] \end{aligned} \quad (9)$$

It is shown that i^{mix} is a function of the driving force $\phi_2^{\text{ocp}} - \phi_1^{\text{ocp}}$ and the exchange current for each reaction. $\phi_2^{\text{ocp}} - \phi_1^{\text{ocp}}$ can be regarded as the sum of overpotential $|\eta_1| + |\eta_2|$ to promote catalytic reactions as applied from the outside. Here, the partitioning of $\phi_2^{\text{ocp}} - \phi_1^{\text{ocp}}$ to the overpotentials $|\eta_1|$ and $|\eta_2|$ can be expressed using Equation (7).

$$|\eta_1| = \phi^{\text{mix}} - \phi_1^{\text{ocp}} = \frac{1}{f} \ln \frac{e^{\alpha f(\phi_2^{\text{ocp}} - \phi_1^{\text{ocp}})} + \frac{(i_1^{I0} + i_1^{II0})}{(i_2^{I0} + i_2^{II0})}}{e^{-(1-\alpha)f(\phi_2^{\text{ocp}} - \phi_1^{\text{ocp}})} + \frac{(i_1^{I0} + i_1^{II0})}{(i_2^{I0} + i_2^{II0})}} \quad (10)$$

$$|\eta_2| = \phi_2^{\text{ocp}} - \phi^{\text{mix}} = \frac{1}{f} \ln \frac{e^{(1-\alpha)f(\phi_2^{\text{ocp}} - \phi_1^{\text{ocp}})} + \frac{(i_2^{I0} + i_2^{II0})}{(i_1^{I0} + i_1^{II0})}}{e^{-\alpha f(\phi_2^{\text{ocp}} - \phi_1^{\text{ocp}})} + \frac{(i_2^{I0} + i_2^{II0})}{(i_1^{I0} + i_1^{II0})}} \quad (11)$$

It should be noted that in Equations (10) and (11) the total overpotential $\phi_2^{\text{ocp}} - \phi_1^{\text{ocp}}$ is partitioned to $|\eta_1|$ and $|\eta_2|$ according to the exchange current or catalytic activity. The crucial factor influencing the overpotential $|\eta_1|$ and $|\eta_2|$ is the ratio of $(i_1^{I0} + i_1^{II0}) : (i_2^{I0} + i_2^{II0})$.

Assuming that a single oxidation reaction and a single reduction reaction take place on each catalyst component (while i_1^{I0} and i_2^{I0} remain, but i_2^{II0} and i_1^{II0} are zero), it is clearly shown in Equations (S2-2) and (S2-3) that the ratio of $i_1^{I0} : i_2^{II0}$ determines the overpotential $|\eta_1|$ and $|\eta_2|$ (See **Supplementary Section 2**). For example, if $i_1^{I0} \ll i_2^{II0}$, $|\eta_1| \gg |\eta_2|$ will be obtained, $|\eta_1|$ and $|\eta_2|$ will approach $\phi_2^{\text{ocp}} - \phi_1^{\text{ocp}}$ and zero, respectively. This example is significant for heterogeneous catalysis because the catalytically difficult reaction 1 with small i_1^{I0} can be promoted by applying larger overpotential of $|\eta_1|$ that corresponds to the total driving force $\phi_2^{\text{ocp}} - \phi_1^{\text{ocp}}$ of the net reaction.

Approximation of overpotential partitioning depending on exchange current

To comprehend the physical meaning of overpotential partitioning, which is the relationship between the overpotential and exchange current, two approximation methods were adopted. One is the Tafel approximation and the other is the linear approximation of the Taylor expansion (See **Supplementary Section 1**) for the currents. In the linear approximation, for the catalyst component I, the currents in Equations (4) and (5) are approximated as follows:

$$i_1^I = i_1^{I0} f(\phi^{\text{mix}} - \phi_1^{\text{ocp}}) \quad (12)$$

$$i_2^I = i_2^{I0} f(\phi^{\text{mix}} - \phi_2^{\text{ocp}}) \quad (13)$$

Again, for the currents on catalyst component II, "I" in Equations (12) and (13) can be replaced by "II." Combining the four equations for currents with Equation (6) yields ϕ^{mix} .

$$\phi^{\text{mix}} = \frac{(i_1^{I0} + i_1^{II0}) \phi_1^{\text{ocp}} + (i_2^{I0} + i_2^{II0}) \phi_2^{\text{ocp}}}{i_1^{I0} + i_1^{II0} + i_2^{I0} + i_2^{II0}} \quad (14)$$

Equation (14) clearly shows that the mixed potential is determined by internal division with a ratio of $(i_1^{I0} + i_1^{II0}) : (i_2^{I0} + i_2^{II0})$. Simultaneously, the current at the mixed potential was obtained as follows:

$$i^{\text{mix}} = (i_1^{I0} + i_1^{II0}) f(\phi^{\text{mix}} - \phi_1^{\text{ocp}}) = \frac{(i_1^{I0} + i_1^{II0})(i_2^{I0} + i_2^{II0})}{i_1^{I0} + i_1^{II0} + i_2^{I0} + i_2^{II0}} (\phi_2^{\text{ocp}} - \phi_1^{\text{ocp}}) \quad (15)$$

i^{mix} corresponds to the apparent catalytic activity in the mixed-potential-driven catalysis, which is determined by exchange current and the driving force of $\phi_2^{\text{ocp}} - \phi_1^{\text{ocp}}$.

In addition, the overpotentials $|\eta_1|$ and $|\eta_2|$ are rewritten using ϕ^{mix} of Equation (14).

$$|\eta_1| = \phi^{\text{mix}} - \phi_1^{\text{ocp}} = \frac{i_2^{I0} + i_2^{II0}}{i_1^{I0} + i_1^{II0} + i_2^{I0} + i_2^{II0}} (\phi_2^{\text{ocp}} - \phi_1^{\text{ocp}}) \quad (16)$$

$$|\eta_2| = \phi_2^{\text{ocp}} - \phi^{\text{mix}} = \frac{i_1^{I^0} + i_1^{II^0}}{i_1^{I^0} + i_1^{II^0} + i_2^{I^0} + i_2^{II^0}} (\phi_2^{\text{ocp}} - \phi_1^{\text{ocp}}) \quad (17)$$

Then, the ratio of the overpotential is expressed by:

$$\begin{aligned} |\eta_1| : |\eta_2| &= \frac{i_2^{I^0} + i_2^{II^0}}{i_1^{I^0} + i_1^{II^0} + i_2^{I^0} + i_2^{II^0}} (\phi_2^{\text{ocp}} - \phi_1^{\text{ocp}}) : \frac{i_1^{I^0} + i_1^{II^0}}{i_1^{I^0} + i_1^{II^0} + i_2^{I^0} + i_2^{II^0}} (\phi_2^{\text{ocp}} - \phi_1^{\text{ocp}}) \\ &= \frac{1}{i_1^{I^0} + i_1^{II^0}} : \frac{1}{i_2^{I^0} + i_2^{II^0}} \end{aligned} \quad (18)$$

Here, it is clear that the driving force of the entire reaction, $\phi_2^{\text{ocp}} - \phi_1^{\text{ocp}}$, is partitioned to overpotential $|\eta_1|$ and $|\eta_2|$ according to the ratio of the sum of the exchange current $i_1^{I^0} + i_1^{II^0}$ and $i_2^{I^0} + i_2^{II^0}$ for reactions 1 and 2, i.e., the catalytic activity. **Fig. 3** is a conceptual electric series circuit representing a mixed-potential-driven catalytic reaction where $\phi_2^{\text{ocp}} - \phi_1^{\text{ocp}}$ corresponds to the electromotive source due to reaction 1 and 2, and $|\eta_1|$ and $|\eta_2|$ corresponds to the overpotentials of reaction 1 and 2 without external electric work. Here, r_1 and r_2 are the so-called charge-transfer resistances depending on the catalytic activity, which are proportional to $1/(i_1^{I^0} + i_1^{II^0})$ and $1/(i_2^{I^0} + i_2^{II^0})$ for the half-reactions 1 and 2, respectively (28, 44). The partitioning of the driving force $\phi_2^{\text{ocp}} - \phi_1^{\text{ocp}}$ into $|\eta_1|$ and $|\eta_2|$ in the mixed-potential-driven catalysis follows the voltage divider rule in the series circuit as $i^{\text{mix}}r_1$ and $i^{\text{mix}}r_2$. This implies that a larger overpotential is partitioned to accelerate processes with a higher charge-transfer resistance.

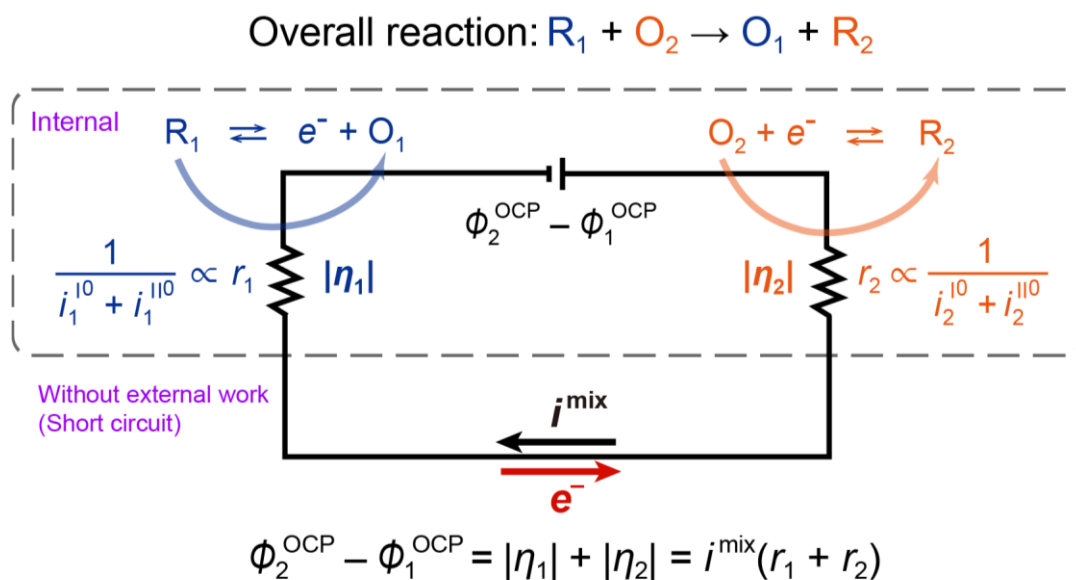


Fig. 3. A conceptual electric series circuit illustrates a mixed-potential-driven catalytic reaction. The internal total voltage $\phi_2^{\text{ocp}} - \phi_1^{\text{ocp}}$ is due to the Gibbs free energy drop $-\Delta G_r$ across the entire mixed-potential-driven catalytic reaction. The charge-transfer resistance (r_1 and r_2), proportional to the reciprocal of the exchange current, plays a role similar to electrical resistors in a circuit. The voltage drops, $i^{\text{mix}}r_1$ and $i^{\text{mix}}r_2$, signifies the overpotentials $|\eta_1|$ and $|\eta_2|$, following

the voltage divider rule. The energy utilized for driving reactions 1 and 2 eventually transforms into Joule heat (ηi).

One can regard this as short circuit where no external work and the Gibbs free energy term is converted to the overpotentials of $|\eta_1|$ and $|\eta_2|$ away from equilibrium. Here, the driving force $\phi_2^{\text{ocp}} - \phi_1^{\text{ocp}}$ corresponds to the Gibbs free energy change ΔG_r of the net reaction with certain concentration of molecules involved at which the reaction proceeds (32, 45, 46).

$$-\Delta G_r = F(\phi_2^{\text{ocp}} - \phi_1^{\text{ocp}}) = F(|\eta_1| + |\eta_2|) \quad (19)$$

This mechanism efficiently drives reactions by utilizing the overpotential to accelerate the forward reaction and decelerate the backward reaction (46). This differs from thermocatalytic reactions, which use a driving force to accelerate both the forward and backward reactions. This is a non-equilibrium steady-state, which is discussed in detail below. However, it is noted here that the energy used to drive reactions 1 and 2 will be dissipated as Joule heat. This dissipated energy is given by Joule's law, which can be expressed as:

$$\begin{aligned} & \eta_1 i_1^{\text{I}} : \eta_1 i_1^{\text{II}} : \eta_2 i_2^{\text{I}} : \eta_2 i_2^{\text{II}} \\ & = \eta_1 \times i_1^{\text{I}0} f \eta_1 : \eta_1 \times i_1^{\text{II}0} f \eta_1 : \eta_2 \times i_2^{\text{I}0} f \eta_2 : \eta_2 \times i_2^{\text{II}0} f \eta_2 \\ & = \frac{i_1^{\text{I}0}}{(i_1^{\text{I}0} + i_1^{\text{II}0})^2} : \frac{i_1^{\text{II}0}}{(i_1^{\text{I}0} + i_1^{\text{II}0})^2} : \frac{i_2^{\text{I}0}}{(i_2^{\text{I}0} + i_2^{\text{II}0})^2} : \frac{i_2^{\text{II}0}}{(i_2^{\text{I}0} + i_2^{\text{II}0})^2} \end{aligned} \quad (20)$$

Equation (20) indicates that the heat generated by each reaction was determined by the exchange current. By contrast, thermochemical reactions directly convert the Gibbs free energy to heat. This distinction is one of the secrets to how mixed-potential-driven catalysis can efficiently accelerate reactions.

Direction of the current flow or electron transfer

In mixed-potential-driven catalysis, the direction of current flow or electron transfer is governed by the exchange current or catalytic activity. Understanding how electrons are transferred between the components is crucial for catalyst design. However, before starting the reaction, the anode and cathode components are unknown. After initiation of the reaction, the magnitude of the exchange current or catalytic activity determines the direction of the current flow or electron transfer and distinguishes between the anode and cathode. Essentially, the roles of Components I and II are uncertain and interchangeable.

This uncertainty leads to three possible cases regarding the direction of the current flow or the designation of components I and II as the anode and cathode of the catalyst, respectively, as shown in **Fig. 4**. Case (A): Overall, the anodic current predominated in component I, and the cathodic current predominated in component II. Case (B): Cathodic current predominates in component I and anodic current predominates in component II. Case (C): Anodic and cathodic currents proceed in pairs in components I and II, respectively, resulting in no current flow between them. By substituting the approximation equations (both the Tafel and linear approximation methods yielded identical results) for the currents of reactions 1 and 2 on components I and II, the direction of the net current in the three cases can be expressed by the exchange currents as follows (see **Supplementary Section 3**):

Case A: $\frac{i_1^{I0}}{i_1^{II0}} > \frac{i_2^{I0}}{i_2^{II0}}$ or $\frac{i_1^{I0}}{i_2^{I0}} > \frac{i_1^{II0}}{i_2^{II0}}$	(21)
Case B: $\frac{i_1^{I0}}{i_1^{II0}} < \frac{i_2^{I0}}{i_2^{II0}}$ or $\frac{i_1^{I0}}{i_2^{I0}} < \frac{i_1^{II0}}{i_2^{II0}}$	(22)
Case C: $\frac{i_1^{I0}}{i_1^{II0}} = \frac{i_2^{I0}}{i_2^{II0}}$ or $\frac{i_1^{I0}}{i_2^{I0}} = \frac{i_1^{II0}}{i_2^{II0}}$	(23)

Equations (21)–(23) indicate that the current flow direction is kinetically governed by the exchange current or catalytic activity ratio. By adjusting the exchange current to control the current direction, researchers can harness the benefits of the internal electric field of the catalyst and enhance selectivity for the desired products.

5

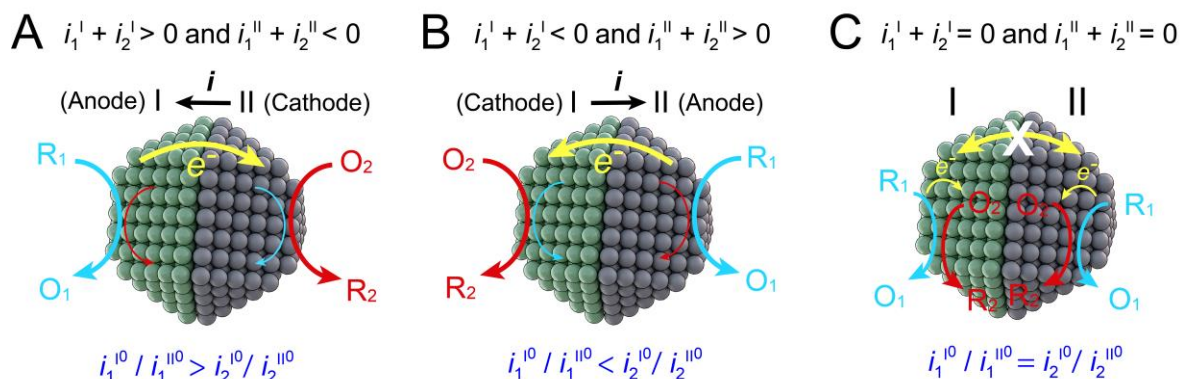


Fig. 4. Direction of the current flow or electron transfer on the catalyst between component I and II occurs through three possible cases. (A) Component I is anode and component II is cathode, i.e., the current flows from II to I; (B) Component I is cathode and component II is anode, i.e., the current flows from I to II; (C) The current flows within both components I and II but there is no current flows between I and II.

10

Non-equilibrium thermodynamics for mixed-potential-driven catalysis at steady-state

Herein, non-equilibrium thermodynamics at steady-state are discussed for mixed-potential-driven catalysis based on the entropy production concept proposed by Prigogine. The starting point of Prigogine's theory is to express the changes in entropy as the sum of two parts:

$$dS = d_e S + d_i S \quad (24)$$

where dS is the total internal variation in the entropy of a system, $d_e S$ is the entropy change of the system owing to the exchange of matter and energy with the exterior, and $d_i S$ is the entropy produced by the irreversible processes inside the system (38). The entropy production term $d_i S$, can serve as a basis for the systematic description of irreversible processes occurring in a system. Moreover, in the steady-state, the total entropy of the system dS remains constant at time dt (38, 47):

$$\frac{dS}{dt} = \frac{d_e S}{dt} + \frac{d_i S}{dt} = 0 \quad \text{or} \quad \frac{d_i S}{dt} = -\frac{d_e S}{dt} \quad (25)$$

For chemical processes in a closed system at constant pressure and temperature, the rate of entropy production can be expressed in the form of Gibbs free energy (38):

$$T \frac{d_i S}{dt} = -\frac{dG_{\text{sys}}}{dt} = -\frac{dG_{\text{sys}}}{d\xi} \frac{d\xi}{dt} = (-\Delta G_r) \frac{d\xi}{dt} \quad (26)$$

where dG_{sys} is the change of total Gibbs free energy of the reaction system, ξ is the extent of reaction, $d\xi/dt$ is the rate of the reaction, and $-\Delta G_r$ is the driving force for the net reaction corresponding to affinity A in Prigogine's textbook (defined as $-dG_{\text{sys}}/d\xi$). In electrical conduction system, the rate of entropy production corresponds to the Joule heat (per unit time) (38, 48, 49):

$$T \frac{d_i S}{dt} = VI = \frac{dQ'}{dt} \quad (27)$$

where V is the potential difference across the entire conductor, I is the convention electric current, and dQ' is the Joule heat generated from the electric current.

The equations above are generally present in textbooks (38, 47–49). Applying these equations to mixed-potential-driven catalysis allows us to describe the energy conversion pathway within the framework of non-equilibrium thermodynamics at steady-state, as follows:

$$T \frac{d_i S}{dt} = -\frac{dG_{\text{sys}}}{dt} = (-\Delta G_r) \frac{d\xi}{dt} = F(\phi_2^{\text{ocp}} - \phi_1^{\text{ocp}}) \frac{d\xi}{dt} = (|\eta_1| + |\eta_2|)i^{\text{mix}} = -T \frac{d_e S}{dt} = \frac{dQ}{dt} \quad (28)$$

where dQ denotes the Joule heat generated due to the reaction. Equation (28) can be illustrated using a closed, isothermal, and isobaric mixed-potential-driven catalytic reaction system at steady-state, as depicted in **Fig. 5**. We may consider that the surroundings of the reaction system are enclosed by rigid adiabatic walls, meaning that the surroundings achieve equilibrium throughout; that is, the temperature, pressure, and chemical potentials remain constant (47). Clearly, the mixed-potential-driven catalysis theory can be categorized as a non-equilibrium theory. Note here that the mixed-potential-driven catalysis provides a mechanism of internal driving force transformation where the Gibbs free energy drop of the net reaction ($-\Delta G_r$) is converted to overpotentials for the two half-reactions ($|\eta_1|$ and $|\eta_2|$) inside the reaction system. Thus, it can be concluded that mixed-potential-driven catalysis converts the Gibbs free energy driving force to internal electric energy and finally to Joule heat.

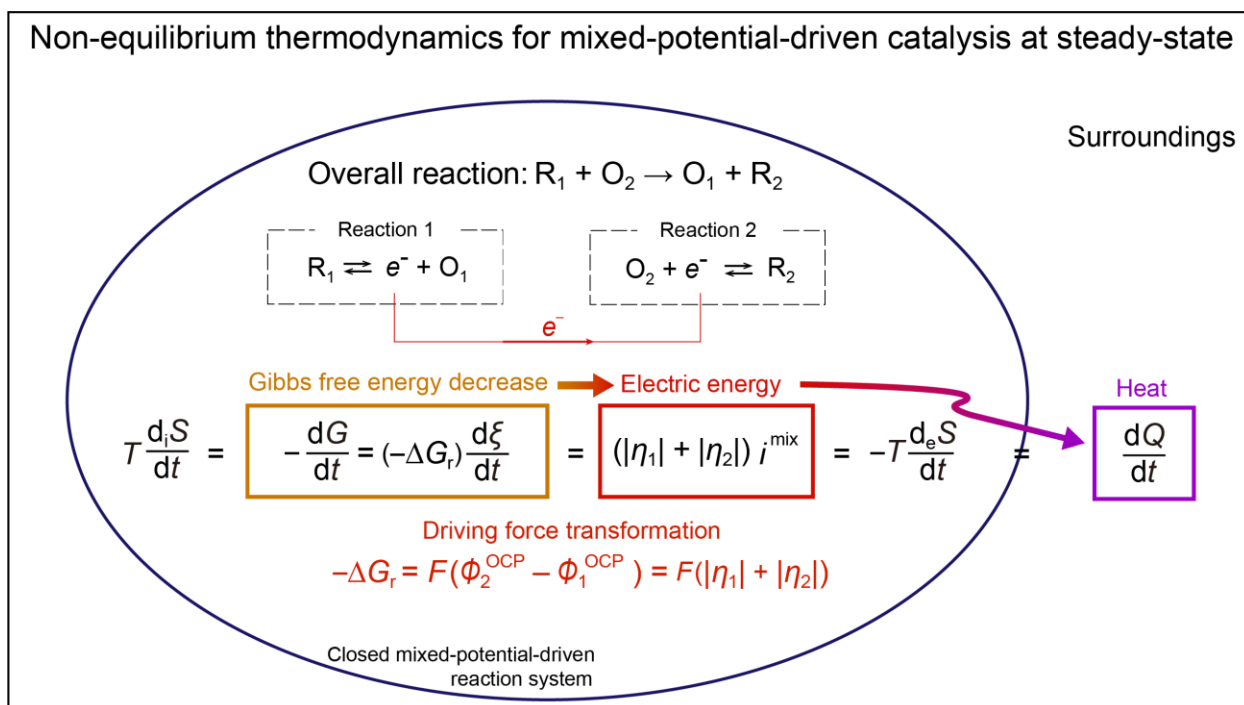


Fig. 5. Steady-state mixed-potential-driven catalysis occurs in a closed, isothermal, and isobaric system. Surroundings are enclosed by rigid adiabatic walls, completely isolated from the external world, a common experimental approximation. At steady-state, the “internal” entropy created in the reaction system ($Td_i S/dt$) which exactly balances the “exchange” entropy to the surroundings ($-Td_e S/dt$), and would be dissipated as heat (dQ/dt) in the surroundings. At any particular time, in mixed-potential-driven catalysis, Gibbs free energy drop of the net reaction ($-\Delta G_r$) undergoes transformation into the overpotentials ($|\eta_1|$ and $|\eta_2|$), which serve to accelerate each of half-reactions, and are ultimately dissipated as Joule heat to the surroundings through the exchange entropy.

Conclusions

Mixed-potential-driven catalysis occurs when the anodic and cathodic reactions are short-circuited in an appropriate electrolyte, and the difference in Gibbs free energy between the anodic and cathodic reactions converts into overpotentials to promote both reactions. In this study, we generalized the theory of mixed-potential-driven catalysis, including the parameters of catalytic activity. Multiple anodic and cathodic reactions occur depending on the catalytic activity, which determines the mixed potential and overpotential. By forming this mixed potential, the Gibbs free energy driving force is converted to an overpotential, and is used to drive the reaction. We formulated the relationship between Gibbs free energy and overpotential using the exchange current density as the catalyst activity. Thus, we clearly demonstrate how the mixed potential is determined, overpotential is partitioned, and anode and cathode are selected by the exchange current. Mixed-potential-driven catalysis theory is categorized as a non-equilibrium theory, as proposed by Prigogine. The theoretical framework developed in this study provides guidelines for researchers to predict and design heterogeneous catalysts, including both thermal and electrochemical processes. Moreover, it is expected to provide a basis for understanding the kinetics and energetics of biological enzymatic reactions that convert the Gibbs free energy drop to overpotential at a steady-state far from equilibrium.

References and Notes

1. Heterogeneous Catalysis. *Nature*. **164**, 50–52 (1949).
2. G. J. Hutchings, Heterogeneous Gold Catalysis. *ACS Cent Sci*. **4**, 1095–1101 (2018).
3. A. T. Bell, Impact of Nanoscience on Heterogeneous Catalysis. *Science*. **299**, 1688–1691 (2003).
4. L. Lin, Y. Ge, H. Zhang, M. Wang, D. Xiao, D. Ma, Heterogeneous Catalysis in Water. *JACS Au*. **1**, 1834–1848 (2021).
5. S. W. Boettcher, Y. Surendranath, Heterogeneous electrocatalysis goes chemical. *Nat Catal*. **4**, 4–5 (2021).
6. G. V. Fortunato, E. Pizzutilo, I. Katsounaros, D. Göhl, R. J. Lewis, K. J. J. Mayrhofer, G. J. Hutchings, S. J. Freakley, M. Ledendecker, Analysing the relationship between the fields of thermo- and electrocatalysis taking hydrogen peroxide as a case study. *Nat Commun*. **13**, 1–7 (2022).
7. D. M. Koshy, S. S. Nathan, A. S. Asundi, A. M. Abdellah, S. M. Dull, D. A. Cullen, D. Higgins, Z. Bao, S. F. Bent, T. F. Jaramillo, Bridging Thermal Catalysis and Electrocatalysis: Catalyzing CO₂ Conversion with Carbon-Based Materials. *Angewandte Chemie - International Edition*. **60**, 17472–17480 (2021).
8. B. N. Zope, D. D. Hibbitts, M. Neurock, R. J. Davis, Reactivity of the gold/water interface during selective oxidation catalysis. *Science*. **330**, 74–78 (2010).
9. J. S. Adams, M. L. Kromer, J. Rodríguez-López, D. W. Flaherty, Unifying Concepts in Electro- and Thermocatalysis toward Hydrogen Peroxide Production. *J Am Chem Soc*. **143**, 7940–7957 (2021).
10. J. Ryu, D. T. Bregante, W. C. Howland, R. P. Bisbey, C. J. Kaminsky, Y. Surendranath, Thermochemical aerobic oxidation catalysis in water can be analysed as two coupled electrochemical half-reactions. *Nat Catal*. **4**, 742–752 (2021).
11. W. C. Howland, J. B. Gerken, S. S. Stahl, Y. Surendranath, Thermal Hydroquinone Oxidation on Co/N-doped Carbon Proceeds by a Band-Mediated Electrochemical Mechanism. *J Am Chem Soc*. **144**, 11253–11262 (2022).
12. X. Huang, O. Akdim, M. Douthwaite, K. Wang, L. Zhao, R. J. Lewis, S. Patisson, I. T. Daniel, P. J. Miedziak, G. Shaw, D. J. Morgan, S. M. Althabhan, T. E. Davies, Q. He, F. Wang, J. Fu, D. Bethell, S. McIntosh, C. J. Kiely, G. J. Hutchings, Au–Pd separation enhances bimetallic catalysis of alcohol oxidation. *Nature*. **603**, 271–275 (2022).
13. L. Zhao, O. Akdim, X. Huang, K. Wang, M. Douthwaite, S. Patisson, R. J. Lewis, R. Lin, B. Yao, D. J. Morgan, G. Shaw, Q. He, D. Bethell, S. McIntosh, C. J. Kiely, G. J. Hutchings, Insights into the Effect of Metal Ratio on Cooperative Redox Enhancement Effects over Au- and Pd-Mediated Alcohol Oxidation. *ACS Catal*. **13**, 2892–2903 (2023).
14. I. Daniel, B. Kim, M. Douthwaite, S. Patisson, R. Lewis, J. Cline, D. Morgan, C. Kiely, S. McIntosh, G. Hutchings, Redox coupling of metals drives rate enhancement in thermochemical oxidative dehydrogenation (2023).
15. K. Takeyasu, Y. Katane, N. Miyamoto, M. Yan, J. Nakamura, Experimental Verification of Mixed-potential-driven Catalysis. *e-Journal of Surface Science and Nanotechnology*. **21**, 164–168 (2022).
16. H. An, G. Sun, M. J. Hülsey, P. Sautet, N. Yan, Demonstrating the Electron-Proton-Transfer Mechanism of Aqueous Phase 4-Nitrophenol Hydrogenation Using Unbiased Electrochemical Cells. *ACS Catal*. **12**, 15021–15027 (2022).
17. C. Wagner, W. Traud, On the interpretation of corrosion processes through the superposition of electrochemical partial processes and on the potential of mixed electrodes. *Corrosion*. **62**, 844–855 (1938).
18. M. Spiro, A. B. Ravno, Heterogeneous Catalysis in Solution. Part II. The Effect of Platinum on Oxidation-Reduction Reactions. *J Chem Soc*, 78–96 (1965).
19. E. Smirnov, P. Peljo, M. D. Scanlon, H. H. Girault, Interfacial Redox Catalysis on Gold Nanofilms at Soft Interfaces. *ACS Nano*. **9**, 6565–6575 (2015).
20. D. Gray, A. Cahill, Theoretical Analysis of Mixed Potentials. *J Electrochem Soc*. **116**, 443 (1969).
21. M. Spiro, Heterogeneous catalysis in solution. Part 17.—Kinetics of oxidation–reduction reaction catalysed by electron transfer through the solid: an electrochemical treatment. *Journal of the Chemical Society, Faraday Transactions 1: Physical Chemistry in Condensed Phases*. **75**, 1507 (1979).
22. D. S. Miller, G. McLendon, Quantitative electrochemical kinetics studies of “microelectrodes”: catalytic water reduction by methyl viologen/colloidal platinum. *J Am Chem Soc*. **103**, 6791–6796 (1981).
23. P. Bindra, J. Roldan, Mechanisms of electroless metal plating. III. Mixed potential theory and the interdependence of partial reactions. *J Appl Electrochem*. **17**, 1254–1266 (1987).
24. G. P. Power, W. P. Staunton, I. M. Ritchie, Mixed potential measurements in the elucidation of corrosion mechanisms-II. Some measurements. *Electrochim Acta*. **27**, 165–169 (1982).

25. M. Spiro, A. B. Ravnö, 15. Heterogeneous catalysis in solution. Part II. The effect of platinum on oxidation–reduction reactions. *J. Chem. Soc.*, 78–96 (1965).
26. A. Mills, Heterogeneous redox catalysts for oxygen and chlorine evolution. *Chem Soc Rev.* **18**, 285–316 (1989).
- 5 27. J. O. M. Bockris, S. U. M. Khan, *Surface Electrochemistry: A Molecular Level Approach* (Springer, 1993).
28. T. Kodera, H. Kita, M. Honda, Kinetic analysis of the mixed potential. *Electrochim Acta.* **17**, 1361–1376 (1972).
29. B. Y. Michael, M. Spiro, Heterogeneous catalysis in solution. Part 22.—Oxidation–reduction reactions catalysed by electron transfer through the solid: theory for partial and complete mass-transport control. *Journal of the Chemical Society, Faraday Transactions 1: Physical Chemistry in Condensed Phases.* **79**, 481–490 (1983).
- 10 30. M. Spiro, P. W. Griffin, Proof of an electron-transfer mechanism by which metals can catalyse oxidation–reduction reactions. *Journal of the Chemical Society D: Chemical Communications*, 262b–263b (1969).
31. H. Zhou, J. H. Park, F. R. F. Fan, A. J. Bard, Observation of single metal nanoparticle collisions by open circuit (Mixed) potential changes at an ultramicroelectrode. *J Am Chem Soc.* **134**, 13212–13215 (2012).
- 15 32. J. O. Bockris, Amulya K. N. Reddy, *Modern Electrochemistry 2B: Electrode in Chemistry, Engineering, Biology and Environmental Science* (Kluwer Academic Publishers, ed. 2, 2001).
33. P. Peljo, M. D. Scanlon, A. J. Olaya, L. Rivier, E. Smirnov, H. H. Girault, Redox Electrocatalysis of Floating Nanoparticles: Determining Electrocatalytic Properties without the Influence of Solid Supports. *Journal of Physical Chemistry Letters.* **8**, 3564–3575 (2017).
- 20 34. D. S. Miller, A. J. Bard, G. McLendon, J. Ferguson, Catalytic Water Reduction at Colloidal Metal “Microelectrodes”. 2. Theory and Experiment. *J Am Chem Soc.* **103**, 5336–5341 (1981).
35. T. de Donder, P. van Rysselberghe, *Thermodynamic Theory of Affinity: A Book of Principles* (Stanford University Press; Milford, Oxford university press, 1936).
- 25 36. W. Nernst, *The new heat theorem: Its foundations in theory and experiment* (Dover Publications, ed. 2, 1969).
37. I. Prigogine, *Introduction to thermodynamics of irreversible processes* (John Wiley & Sons, ed. 3, 1968).
38. D. Kondepudi, I. Prigogine, *Modern Thermodynamics: From Heat Engines to Dissipative Structures* (John Wiley & Sons, 1998).
- 30 39. L. A. Smith, M. W. Glasscott, K. J. Vannoy, J. E. Dick, Enzyme Kinetics via Open Circuit Potentiometry. *Anal Chem.* **92**, 2266–2273 (2020).
40. K. Cammann, G. A. Rechnitz, Exchange Kinetics at Ion-Selective Membrane Electrodes. *Anal Chem.* **48**, 856–862 (1976).
41. W. C. Kao, T. Kleinschroth, W. Nitschke, F. Baymann, Y. Neehaul, P. Hellwig, S. Richers, J. Vonck, M. Bott, C. Hunte, The obligate respiratory supercomplex from Actinobacteria. *Biochim Biophys Acta Bioenerg.* **1857**, 1705–1714 (2016).
- 35 42. S. Freguia, B. Viridis, F. Harnisch, J. Keller, Bioelectrochemical systems: Microbial versus enzymatic catalysis. *Electrochim Acta.* **82**, 165–174 (2012).
43. A. M. Bertholet, Y. Kirichok, Mitochondrial H Leak and Thermogenesis. *Annu Rev Physiol.* **84**, 381–407 (2022).
- 40 44. A. J. Bard, L. R. Faulkner, *Electrochemical Methods: Fundamentals and Applications* (John Wiley & Sons, ed. 2, 2001).
45. L. Lazzari, "General aspects of corrosion" in *Encyclopaedia of Hydrocarbons* (Eni: Istituto della Enciclopedia italiana, 2005), pp. 485–505.
46. R. O’Hayre, S.-W. Cha, W. Colella, F. B. Prinz, *Fuel cell fundamentals* (John Wiley & Sons, 2016).
47. S. R. Caplan, A. Essig, *Bioenergetics and Linear Nonequilibrium Thermodynamics: The Steady State* (Harvard University Press, 1983).
48. J. Newman, N. P. Balsara, *Electrochemical Systems* (John Wiley & Sons, New Jersey, 2004).
- 50 49. J. O. Bockris, B. E. Conway, E. Yeager, R. E. White, Eds., *Comprehensive Treatise of Electrochemistry Volume 3: Electrochemical Energy Conversion and Storage* (Plenum Publishing Corporation, 1981).
50. M. Boudart, G. Djega-Mariadassou, *Kinetics of Heterogeneous Catalytic Reactions* (Princeton University Press, New Jersey, 1984).

Acknowledgments:

55 MY, KT, JN, NAPN thank Prof. Hiroaki Suzuki for fruitful discussions on the mixed potential.

Funding:

This work was supported by JSPS Grant-in-Aid for Scientific Research (KAKENHI) Grant Number 23H05459, JST the establishment of university fellowships towards the creation of science technology innovation Grant Number JPMJFS2106, Project for University-Industry Cooperation Strengthening in Tsukuba, and TRiSTAR Program, a Top Runner Development Program Engaging Universities, National Labs, and Companies.

Author contributions:

Conceptualization: JN

Data Curation: MY, KT

Formal Analysis: MY, KT

Funding Acquisition: MY, KT, JN

Investigation: MY, KT, JN, NAPN

Methodology: MY, KT, JN

Project administration: JN

Supervision: KT, JN

Validation: MY, KT, JN

Visualization: MY, KT, JN, NAPN

Writing – original draft: MY, KT, JN

Writing – review & editing: MY, KT, JN, NAPN

Competing interests: Authors declare that they have no competing interests.

Data and materials availability: All data are available in the main text or the supplementary materials.

Supplementary Materials

Supplementary Text

Figs. S1 to S4

Tables S1

References (12, 15, 16, 27, 32, 35, 37–39, 43–45, 50)